Kinetics of Emulsion Copolymerization. II. Effect of Free Radical Desorption on the Rate of Emulsion Copolymerization of Styrene and Methyl Methacrylate

M. NOMURA, K. YAMAMOTO, I. HORIE, and K. FUJITA, *Department of Industrial Chemistry, Fukui University, Fukui, Japan* and M. HARADA, *Atomic Energy Institute, Kyoto University, Uji, Japan*

Synopsis

The rate coefficient for radical desorption from the polymer particles is derived for an emulsion copolymerization system, assuming, for simplicity, that only monomer radicals can desorb from the particles. The effect of free radical desorption on the rate of emulsion copolymerization and the copolymer composition is theoretically analyzed, using the rate coefficient for radical desorption developed in this paper and a mathematical reaction model proposed earlier by the present authors for an emulsion copolymerization system where the average number of total radicals per particle does not exceed 0.5. The validity of the analysis is demonstrated experimentally using the seeded emulsion copolymerization of styrene (ST) and methyl methacrylate (MMA). Radical desorption from the particles does not affect the copolymer composition, but the desorption of MMA—monomer radicals plays an important role in determining the rate of emulsion copolymerization, while the desorption of ST—monomer radicals from the particles can be neglected from a kinetic point of view.

INTRODUCTION

In published studies on emulsion copolymerization, the main interest has been on explaining the copolymer composition and the differences in composition formed in emulsion vs. bulk copolymerization systems. Thus, the rate of emulsion copolymerization has received scant attention in the literature in spite of its industrial importance. Recently, Lin et al.[1] studied the kinetics of emulsion copolymerization of styrene and acrylonitrile in an azeotropic composition using our reaction model[2] for an emulsion copolymerization system. Ballard et al.[3] also proposed a mathematical model for an emulsion copolymerization system which can predict the time evolution of the copolymer composition and copolymer sequence distribution. However, their model is rather complex for predicting the rate of emulsion copolymerization and the average copolymer composition.

The rate of emulsion homopolymerization is greatly affected by radical desorption from the particles.[4–7] This is also true for emulsion copolymerization systems because the mechanism of emulsion copolymerization is essentially the same as that of emulsion homopolymerization. As long as the value of the rate coefficient for radical desorption in an emulsion copolymerization system cannot be estimated quantitatively, the rate of emulsion copolymerization cannot be predicted. To date, however, there have been no works which deal with the rate coefficient for radical desorption in an emulsion copolymerization system, though several papers have recently appeared which derive it for an emulsion homopolymerization system.[5–9]

Journal of Applied Polymer Science, Vol. 27, 2483–2501 (1982)
 CCC 0021-8995/82/072483-19$02.90

In this paper, the rate coefficient for radical desorption from the particles is derived for an emulsion copolymerization system, and then the effect of radical desorption on the rate of emulsion copolymerization and the copolymer composition is examined theoretically and experimentally using our mathematical reaction model[2] developed for an emulsion copolymerization system and the seeded emulsion copolymerization of styrene (ST) and methyl methacrylate (MMA).

THEORY

Mathematical Reaction Model for an Emulsion Copolymerization System[2]

Although our reaction model has been briefly introduced by Lin et al.,[1] its derivation is explained in more detail. Let us consider an emulsion copolymerization system where two comonomers, A and B, are copolymerized. For simplicity, the following five assumptions are made: (i) Polymer particles contain at most one radical; (ii) only monomer radicals can desorb from and reenter into the particles; (iii) no discrimination is made between the radicals with or without an initiator fragment on its end; (iv) instantaneous termination occurs when another radical enters the particle that already contains a radical; and (v) propagation, termination, and chain transfer reactions in the water phase can be neglected from a kinetic point of view. Under these assumptions, we can establish the following set of differential equations for the respective species in the batch reactor, using the reaction rate expressions (Table I). Furthermore, we apply the steady state hypothesis to these differential equations. Thus, we have the following.

(I) Initiator concentration $[I]_w$ and radical production rate r_i in the water phase:

$$\frac{d[I]_w}{dt} = -k_d[I]_w \tag{1}$$

Integration of Eq. (1) yields

$$[I]_w = [I_0]_w \exp(-k_d t) \tag{1'}$$

The rate of radical production in the water phase is represented by

$$r_i = 2k_d f[I]_w \tag{2}$$

(II) The concentration of initiator radicals in the water phase $[I^*]_w$:

$$\frac{d[I^*]_w}{dt} = r_i + k_{fI}N_I^* - k_{eI}[I^*]_w N_T = 0 \tag{3}$$

(III) The concentration of A-monomer radicals in the water phase $[M_a^*]_w$:

$$\frac{d[M_a^*]_w}{dt} = k_{fa}N_a^* - k_{ea}[M_a^*]_w N_T = 0 \tag{4}$$

(IV) The concentration of B-monomer radicals in the water phase $[M_b^*]_w$:

$$\frac{d[M_b^*]_w}{dt} = k_{fb}N_b^* - k_{eb}[M_b^*]_w N_T = 0 \tag{5}$$

TABLE I
Elementary Reactions and Their Rates

Reaction scheme	Reaction rate
(1) Initiation of radicals in the water phase	
$I \rightarrow 2I_w^*$	$r_i = 2k_d f[I]_w$ (T-1)
(2) Entry of radicals into particles from the water phase	
(i) Instantaneous termination	
$N^* + I_w^* \rightarrow N_0$	$r_{eI} = k_{eI}[I^*]_w N^*$ (T-2)
$N^* + M_{aw}^* \rightarrow N_0$	$r_{ta} = k_{ea}[M_a^*]_w N^*$ (T-3)
$N^* + M_{bw}^* \rightarrow N_0$	$r_{tb} = k_{eb}[M_b^*]_w N^*$ (T-4)
(ii) Activation of particle	
$N_0 + I_w^* \rightarrow N_I^*$	$r_{eI} = k_{eI}[I^*]_w N_0$ (T-5)
$N_0 + M_{aw}^* \rightarrow N_a^*$	$r_{ea} = k_{ea}[M_a^*]_w N_0$ (T-6)
$N_0 + M_{bw}^* \rightarrow N_b^*$	$r_{eb} = k_{eb}[M_b^*]_w N_0$ (T-7)
(3) Initiation reaction in particles	
$I_p^* + M_{ap} \rightarrow M_{ap}^*$	$r_{ia} = k_{ia}[M_a]_p N_I^*$ (T-8)
$I_p^* + M_{bp} \rightarrow M_{bp}^*$	$r_{ib} = k_{ib}[M_b]_p N_I^*$ (T-9)
(4) Propagation reaction in particles	
$P_{ap}^* + M_{ap} \rightarrow P_{ap}^*$	$r_{paa} = k_{paa}[M_a]_p N_a^*$ (T-10)
$P_{bp}^* + M_{ap} \rightarrow P_{ap}^*$	$r_{pba} = k_{pba}[M_a]_p N_b^*$ (T-11)
$P_{ap}^* + M_{bp} \rightarrow P_{bp}^*$	$r_{pab} = k_{pab}[M_b]_p N_a^*$ (T-13)
$P_{bp}^* + M_{bp} \rightarrow P_{bp}^*$	$r_{pbb} = k_{pbb}[M_b]_p N_b^*$ (T-14)
(5) Chain transfer to monomer in particles	
$P_{ap}^* + M_{ap} \rightarrow P + M_{ap}^*$	$r_{faa} = k_{maa}[M_a]_p N_a^*$ (T-15)
$P_{bp}^* + M_{ap} \rightarrow P + M_{ap}^*$	$r_{fba} = k_{mba}[M_a]_p N_b^*$ (T-16)
$P_{ap}^* + M_{bp} \rightarrow P + M_{bp}^*$	$r_{fab} = k_{mab}[M_b]_p N_a^*$ (T-17)
$P_{bp}^* + M_{bp} \rightarrow P + M_{bp}^*$	$r_{fbb} = k_{mbb}[M_b]_p N_b^*$ (T-18)
(6) Desorption of radicals from particles:	
$N_I^* \rightarrow N_0 + I_w^*$	$r_{dI} = k_{fI} N_I^*$ (T-19)
$N_a^* \rightarrow N_0 \rightarrow M_{aw}^*$	$r_{da} = k_{fa} N_a^*$ (T-20)
$N_b^* \rightarrow N_0 + M_{bw}^*$	$r_{db} = k_{fb} N_b^*$ (T-21)

(V) The number of polymer particles containing an initiator radical N_I^*:

$$\frac{dN_I^*}{dt} = k_{eI}[I^*]_w N_0 - (k_{ia}[M_a]_p + k_{ib}[M_b]_p)N_I^* - (k_{ea}[M_a^*]_w + k_{eb}[M_b^*]_w + k_{eI}[I^*]_w)N_I^* - k_{fI}N_I^* = 0 \quad (6)$$

(VI) The number of polymer particles containing an A-radical N_a^*:

$$\frac{dN_a^*}{dt} = k_{ia}[M_a]_p N_I^* + k_{ea}[M_a^*]_w N_0 + (k_{pba} + k_{mba})[M_a]_p N_b^* - (k_{pab} + k_{mab})[M_b]_p N_a^* - (k_{ea}[M_a^*]_w + k_{eb}[M_b^*]_w + k_{eI}[I^*]_w)N_a^* - k_{fa}N_a^* = 0 \quad (7)$$

(VII) The number of polymer particles containing a B-radical N_b^*:

$$\frac{dN_b^*}{dt} = k_{ib}[M_b]_p N_I^* + k_{eb}[M_b^*]_w N_0 + (k_{pab} + k_{mab})[M_b]_p N_a^* - (k_{pba} + k_{mba})[M_a]_p N_b^* - (k_{ea}[M_a^*]_w + k_{eb}[M_b^*]_w + k_{eI}[I^*]_w)N_b^* - k_{fb}N_b^* = 0 \quad (8)$$

(VIII) The rate of emulsion copolymerization in the particles R_p:

$$\text{for A monomer,} \quad R_{pa} = -\frac{dM_a}{dt} = k_{paa}[M_a]_p N_a^* + k_{pba}[M_a]_p N_b^* \quad (9)$$

$$\text{for B monomer,} \quad R_{pb} = -\frac{dM_b}{dt} = k_{pbb}[M_b]_p N_b^* + k_{pab}[M_b]_p N_a^* \quad (10)$$

Thus, the total rate of emulsion copolymerization R_{pt} is given by

$$R_{pt} = R_{pa} + R_{pb} \tag{11}$$

(IX) The composition of copolymers produced in an emulsion copolymerization: From Eqs. (9) and (10), we have

$$\frac{dM_a}{dM_b} = \frac{k_{paa}[M_a]_p N_a^* + k_{pba}[M_b]_p N_b^*}{k_{pbb}[M_b]_p N_b^* + k_{pab}[M_b]_p N_a^*} = \left(\frac{[M_a]_p}{[M_b]_p}\right)\left(\frac{\gamma_a[M_a]_p + [M_b]_p}{\gamma_b[M_b]_p + [M_a]_p}\right) \tag{12}$$

Equation (12) expresses the mole ratio of copolymers instantaneously produced in emulsion copolymerization, and is the same as the "Mayo–Lewis equation." Furthermore, the desorption of radicals from the particles does not affect the copolymer composition, because eq. (12) does not involve the rate coefficient for radical desorption from the particles, k_f.

By introducing eqs. (3), (4), and (5) into eq. (7), eq. (7) is rewritten as

$$\frac{dN_a^*}{dt} = k_{ia}[M_a]_p N_I^* + (k_{pba} + k_{mba})[M_a]_p N_b^* - (k_{pab} + k_{mab})[M_b]_p N_a^* - \left[2k_{fa}\left(\frac{N_a^*}{N_T}\right) + (k_{fa} + k_{fb})\left(\frac{N_b^*}{N_T}\right) + \frac{r_i}{N_T}\right] N_a^* = 0 \tag{7'}$$

In eq. (7'), the value of N_I^* is much less than those of N_a^* and N_b^*, because initiator radicals are so reactive that initiation reaction occurs instantaneously when they enter the particles. Furthermore, the values of propagation rate constants are much greater than those of chain transfer rate constant and the rate coefficient for radical desorption shown later. Hence, eq. (7') is simplified with good accuracy as:

$$k_{pba}[M_a]_p N_b^* = k_{pab}[M_b] N_a^* \tag{13}$$

This equation can be also derived from eq. (8).

By adding eqs. (6), (7), and (8), and inserting eqs. (3), (4), and (5), we have

$$(k_{fa}N_a^* + k_{fb}N_b^* + k_{fI}N_I^* + r_i/N_T)(1 - 2N^*) - (k_{fa}N_a^* + k_{fb}N_b^* + k_{fI}N_I^*) = 0 \tag{14}$$

where

$$N^* = N_a^* + N_b^* + N_I^* \tag{15}$$

The average number of respective radicals per particle are defined by

$$\bar{n}_a = N_a^*/N_T, \quad \bar{n}_b = N_b^*/N_T, \quad \bar{n}_I = N_I^*/N_T, \quad \text{and} \quad \bar{n}_t = (N_a^* + N_b^* + N_I^*)/N_T \tag{16}$$

Considering that $N_a^*, N_b^* \gg N_I^*$, that is, $\bar{n}_a, \bar{n}_b \gg \bar{n}_I$, eqs. (13)–(15) are simplified and rewritten as

$$k_{pba}[M_a]_p \bar{n}_b = k_{pab}[M_b]_p \bar{n}_a \tag{13'}$$

$$(k_{fa}\bar{n}_a + k_{fb}\bar{n}_b + r_i/N_T)(1 - 2\bar{n}_t) - (k_{fa}\bar{n}_a + k_{fb}\bar{n}_b) = 0 \tag{14'}$$

where

$$\bar{n}_t = \bar{n}_a + \bar{n}_b + \bar{n}_I \cong \bar{n}_a + \bar{n}_b \tag{15'}$$

Solving eqs. (13')–(15') for $\bar{n}_a$ and $\bar{n}_b$, we have

$$\bar{n}_a = \left(\frac{1}{1 + A}\right)\bar{n}_t, \quad \bar{n}_b = \left(\frac{A}{1 + A}\right)\bar{n}_t \tag{17}$$

$$\bar{n}_t = \tfrac{1}{2}[-(CD) + \sqrt{(CD)^2 + 2(CD)}] \tag{18}$$

where

$$A = \frac{\bar{n}_b}{\bar{n}_a} = \left(\frac{k_{paa}}{k_{pbb}}\right)\left(\frac{\gamma_a}{\gamma_b}\right)\left(\frac{[M_b]_p}{[M_a]_p}\right), \quad B = \frac{k_{fb}}{k_{fa}} \quad (k_{fa} \neq 0)$$

$$C = \frac{r_i}{k_{fa}N_T}, \quad D = \left(\frac{1+A}{1+AB}\right).$$

On the other hand, we can obtain an expression similar to eq. (18) by following treatment.[10] In eq. (14′), we define the average rate coefficient for radical desorption from the particles, $\bar{k}_f$, by

$$\bar{k}_f\bar{n}_t = k_{fa}\bar{n}_a + k_{fb}\bar{n}_b \tag{19}$$

Substitution of eq. (17) into eq. (19) yields

$$\bar{k}_f = \left(\frac{1}{1+A}\right)k_{fa} + \left(\frac{A}{1+A}\right)k_{fb} \tag{20}$$

From eqs. (14′) and (20), we have

$$\bar{n}_t = \tfrac{1}{2}[-\mathbf{C} + \sqrt{\mathbf{C}^2 + 2\mathbf{C}}], \quad \mathbf{C} = r_i/\bar{k}_f N_T \tag{21}$$

Equations (9) and (10) representing the rate of emulsion copolymerization are simplified, by using eqs. (16) and (13′), as

$$R_{pa} = -dM_a/dt = (k_{paa}[M_a]_p\bar{n}_a + k_{pba}[M_a]_p\bar{n}_b)N_T$$
$$= k_{paa}([M_a]_p + [M_a]_p/\gamma_a)\bar{n}_a N_T \tag{22}$$

$$R_{pb} = -dM_b/dt = (k_{pbb}[M_b]_p\bar{n}_b + k_{pab}[M_b]_p\bar{n}_a)N_T$$
$$= k_{pbb}([M_b]_p + [M_b]_p/\gamma_b)\bar{n}_b N_T \tag{23}$$

Thus, we can predict the rate of emulsion copolymerization consisting of two comonomers A and B, if the values of the rate coefficient for radical desorption from the particles k_{fa} and k_{fb} can be estimated.

Derivation of the Rate Coefficient for Radical Desorption, k_f, for Emulsion Copolymerization Systems

The present authors[6,8,9] have already derived the rate coefficient for radical desorption from the particles for an emulsion homopolymerization system by deterministic and stochastic approaches. By applying the same approaches, we can obtain the rate coefficient for radical desorption for an emulsion copolymerization system. In this paper, the stochastic approach is applied.

A radical in the polymer particles will probably undergo the following four events that will occur in the particles: (i) initiation and propagation reactions (ii) chain transfer to monomer, polymer, emulsifier, and so on, (iii) termination reaction when another radical enters the particle which contains a radical, and (iv) desorption from the particle into the water phase. The production rate of A-monomer radicals by chain transfer of A- and B-polymer radicals to A-monomer can be represented by

$$k_{maa}[M_a]_p N_a^* + k_{mba}[M_a]_p N_b^* \tag{24}$$

Part of these radicals will escape from the particles before adding one monomer unit, and that fraction is given by

$$\Phi_{Ma}[k_{maa}[M_a]_p N_a^* + k_{mba}[M_a]_p N_b^*] \tag{25}$$

where Φ_{Ma} is the probability of A-monomer radicals escaping from the polymer particles before adding one monomer unit.

At steady state, the concentration of A-monomer radicals in the water phase is constant because we assumed that termination reaction in the water phase could be neglected from a kinetic point of view, and hence the rates of desorption and absorption of A-monomer radicals in the particles should be the same. Therefore, the decrease, due to radical desorption, in the number of polymer particles containing an A-monomer radical is partly recovered by the entry of A-monomer radicals from the water phase into the particles containing no radicals. Let N_{am} be the number of polymer particles containing an A-monomer radical. Then, $K_{0a}N_{am}$ represents the desorption rate of A-monomer radicals, i.e., the rate of decrease in the number of polymer particles containing an A-monomer radical. $K_{0a}N_{am}(N_0/N_T)$ expresses the rate of recovery of the number of polymer particles containing an A-monomer radical due to the entry of A-monomer radicals. Therefore, the apparent (or net) rate of desorption of A-monomer radicals per particle containing an A-monomer radical is given by

$$[K_{0a}N_{am} - K_{0a}N_{am}(N_0/N_T)]/N_{am} \cong K_{0a}(N_a^* + N_b^*)/N_T \cong K_{0a}\bar{n}_t \tag{26}$$

In eq. (2b), K_{0a} indicates the desorption rate constant for A-monomer radicals and can be obtained by applying the diffusion theory as follows[8,9]:

$$K_{0a} = K_{sa}(a_p/v_p) = 12D_{wa}\delta_a/m_{da}d_p^2 \tag{27}$$

where K_{sa} is the overall mass-transfer coefficient across the interface between the particle and water phases, d_p, a_p, and v_p are the diameter, surface area, and volume of a particle, respectively, D_{wa} is the diffusion coefficient of A-monomer radicals in the water phase, δ_a is the ratio of water-side film-mass-transfer resistance to overall mass-transfer resistance for A-monomer radicals defined by[8,9]

$$\delta_a = [1 + (2D_{wa}/m_{da}D_{pa})]^{-1} \tag{28}$$

D_{pa} is the diffusion coefficient of A-monomer radicals in the polymer particles, and m_{da} is the partition coefficient for A-monomer radicals between the particle and water phase defined by

$$[M_a^*]_p = m_{da}[M_a^*]_w \tag{29}$$

Considering the rate for each event (i)–(iv) to occur, only events (i) and (iv) are usually important for calculating the probability Φ_{Ma}. The probability Φ_{Ma} is, therefore, represented by

$$\Phi_{Ma} = \frac{K_{0a}\bar{n}_t}{K_{0a}\bar{n}_t + (k_{paa}[M_a]_p + k_{pab}[M_b]_p)} \tag{30}$$

In eq. (30), however, if the desorbed radicals do not reenter the particles, for example, due to termination reaction in the water phase, it is apparent from eq. (26) that $K_{0a}\bar{n}_t$ in eq. (30) should be replaced by K_{0a}. The quantity given by eq. (25) expressses the apparent (or net) rates of radical desorption from the particles. However, the rate coefficient for radical desorption, k_{fa}, is the coefficient which is related to the true rate of desorption of A-monomer radicals from the particles. By using the rate coefficient, k_{fa}, the apparent (or net) rate of

desorption of A-monomer radicals from the particles containing A-radicals, which is given by Eq. (25), can be represented by

$$k_{fa}N_a^* - k_{fa}N_a^*(N_0/N_T) = \Phi_{Ma}(k_{maa}[M_a]_p N_a^* + k_{mba}[M_a]_p N_b^*) \quad (31)$$

Introduction of eq. (30) into eq. (31) and rearrangement yield

$$k_{fa} = K_{0a}\left(\frac{k_{maa}[M_a]_p + k_{mba}[M_a]_p(\bar{n}_b/\bar{n}_a)}{K_{0a}\bar{n}_t + k_{paa}[M_a]_p + k_{pab}[M_b]_p}\right) \quad (32)$$

At steady state, $\bar{n}_b/\bar{n}_a$ is given by eq. (13′). Thus, by introducing eq. (13′) into eq. (32), we have

$$k_{fa} = K_{0a}\left(\frac{\gamma_a C_{maa}[M_a]_p + C_{mba}[M_b]_p}{\gamma_a[[M_a]_p + (K_{0a}\bar{n}_t/k_{paa})] + [M_b]_p}\right) \quad (33)$$

In the same manner, we can obtain the rate coefficient for desorption of B-monomer radicals from the particles, k_{fb}, as follows:

$$k_{fb} = K_{0b}\left(\frac{\gamma_b C_{mbb}[M_b]_p + C_{mab}[M_a]_p}{\gamma_b[[M_b]_p + (K_{0b}\bar{n}_t/k_{pbb})] + [M_a]_p}\right) \quad (34)$$

EXPERIMENTAL

To clarify experimentally the effect of radical desorption from the particles on the rate of emulsion copolymerization, the seeded emulsion copolymerization of styrene (ST) and methyl methacrylate (MMA) was carried out and was analyzed using the rate coefficient for radical desorption and the mathematical reaction model given above.

Materials

Commercially available MMA monomer inhibited with hydroquinone was first washed with saturated $NaHSO_3$ solution and then with 5% NaOH solution, while ST monomer of commercial grade was washed with 15% KOH solution to remove inhibitor. The treated monomers were washed further with deionized water, distilled twice under reduced nitrogen pressure, and stored at −20°C in a refrigerator. Potassium persulfate and sodium lauryl sulfate of extra-pure grade were used as initiator and emulsifier, respectively, without further purification. All water used was purified by distillation in the presence of alkaline potassium permanganate.

Apparatus and Experimental Procedure

The seeded emulsion copolymerization of ST and MMA was carried out using the same experimental apparatus as shown previously.[11] The reactor was a 400-cm^3 cylindrical glass vessel with a dished bottom, equipped with a four-bladed paddle type impeller. Four baffle plates were set on the vessel wall at 90° intervals to improve mixing of the reaction mixture. The polymerizations were started as follows: The reactor vessel was charged with the desired amount of seed latex, purified water, monomers, and a small amount of sodium lauryl sulfate emulsifier to prevent coagulation of latex particles. The oxygen dissolved

in the reaction mixture was purged by bubbling pure nitrogen gas (purity 99.995%) through the reaction mixture for about half an hour. The polymerization was started by injecting aqueous initiator solution in a dropping funnel, which had been previously deoxygenized with a pure nitrogen gas, into the reactor. All the polymerizations were carried out at 50 ± 0.5°C with the use of a thermostated water bath under a high purity nitrogen atmosphere. Impeller speeds were kept constant at 400 rpm. Total monomer conversion was determined gravimetrically using methanol as precipitant.

Seed Latex

Seed latex used in this experiment was made in the same apparatus and conditions as used for the seeded emulsion copolymerization experiments. The average particle size, particle concentration, and the copolymer composition in the seed latex particles were controlled by changing initial emulsifier and monomer concentrations, and comonomer composition in the monomer feed. Polymerizations were completed until nearly no residual monomers could be detected. The latex thus produced (80 cc) was then washed with purified water (500 cc) through a Pellicon filter with a nominal molecular weight limit of 1,000 (PSAC 047 10) to remove the residual emulsifier and initiator in the water phase.[12] The washed seed latex was stored in a refrigerator at 5°C for use.

Measurement of Particle Number

The number of polymer particles was determined from the total monomer conversion X_{Mt} and the volume average diameter of the particles, $\bar{d}_p$, which was measured by electron microscopy:

$$\bar{d}_p = (\sum n_i d_{pi}^3 / \sum n_i)^{1/3} \tag{35}$$

$$N_T = 6M_0 X_{Mt} / \pi \bar{d}_p^3 \rho_p \tag{36}$$

The constancy of the number of polymer particles during the polymerization was checked by measuring it before and after the polymerization; the amount of emulsifier added to prevent coagulation of latex particles was very small so that no new particles formed during the polymerization.

Measurement of Monomer Concentration in Monomer-Swollen Particles

The concentration of each monomer in the monomer-swollen particles was determined by the following procedure: The monomer droplets in the sample withdrawn from the reaction vessel were separated as soon as possible with a centrifuge. After removing the separated monomer layer from the sample, the treated sample was poured into methanol. The precipitated polylmers were filtered off, and the filtrate was subjected to the measurement of monomer content by gas chromatography. In calculating the concentration of each monomer in the monomer-swollen particles, the volumes of monomers and polymers in the particles were assumed to be additive.

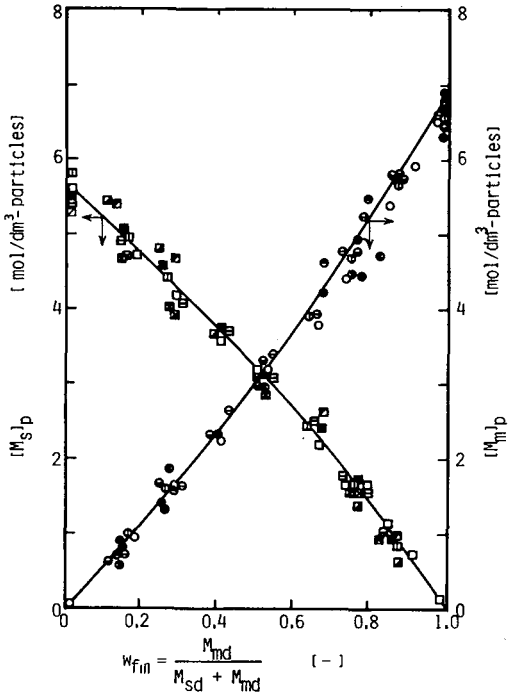

Fig. 1(a). Effects of particle size and copolymer composition in seed polymer particles on concentration of each monomer in monomer-swollen polymer particles. Temp = 50°C; ionic strength: $\mu \approx 0$; interfacial tension: $\sigma = 57$ dyn/cm.

Key

$[M_m]_p$	$[M_s]_p$	$P_m/(P_m + P_s)$	d_p (nm)
●	■	1.0	90
⊖	⊟	0.85	75
⊕	⊞	0.70	80
◐	◘	0.50	55
◓	◩	0.10	90
◒	◪	0	80
⊗	⊠	0.50	25
⊛	▣	0.50	110

EXPERIMENTAL RESULTS AND DISCUSSION

Monomer Concentration in Monomer-Swollen Particles

In emulsion homopolymerization the monomer concentration in the monomer-swollen polymer particles is affected by many factors such as particle size, additives, and the interfacial tension between the particle surface and the water phase. In this experiment, therefore, the effects of particle size, interfacial tension, copolymer composition in the particles, ionic strength, and comonomer composition in the monomer feed on the concentration of each monomer in the particles was examined. Figure 1(a) shows the effects of particle size and copolymer composition in the particles, the abscissa being the weight fraction of MMA-monomer in the monomer droplets which are in equilibrium with the

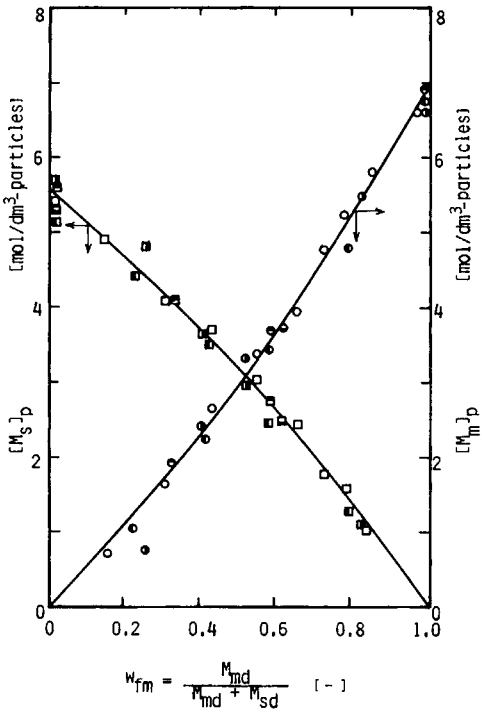

Fig. 1(b). Effect of ionic strength and interfacial tension in water phase on concentration of each monomer in monomer-swollen polymer particles. Seed particles used: d_p = 75 nm (dry basis); $P_m/(P_m + P_s)$ = 0.85. Temp = 50°C.

Key

$[M_m]_p$	$[M_s]_p$	μ	σ
○	□	0	57
◑	□	0.02	57
◐	□	0.12	57
◒	■	0	47
◓	■	0	40

monomer-swollen polymer particles. Figure 1(b) shows the effects of ionic strength in the water phase and interfacial tension between the particle and water phases. The ionic strength and interfacial tension were changed by changing the amounts of K_2SO_4 and sodium lauryl sulfate added, respectively. The concentrations of each monomer in the particle are determined by the monomer composition in the monomer droplets, and are a very weak function of particle size, copolymer composition in the particles, ionic strength, and interfacial tension. The solid lines (Fig. 1) represent the values calculated from the following empirical equations and show good agreement with experimental values:

$$[M_s]_p = 22.4\left(\frac{1 - w_{fm}}{4 - w_{fm}}\right) \tag{37}$$

$$[M_m]_p = 27.6\left(\frac{w_{fm}}{5 - w_{fm}}\right) \tag{38}$$

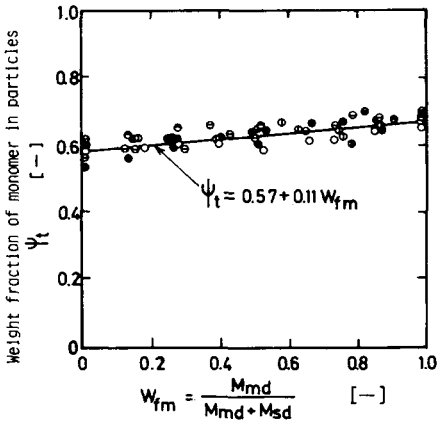

Fig. 2. Effect of monomer composition in monomer droplets on weight fraction of monomer in monomer-swollen polymer particles. Key same as in Figure 1(a). Temp = 50°C.

where

$$w_{fm} = \frac{M_{md}}{M_{md} + M_{sd}} \tag{39}$$

w_{fm} represents the weight fraction of MMA-monomer in the monomer droplets. Considering that the molecular weights of MMA and ST are almost the same, w_{fm} approximately expresses the mole fraction of MMA monomer in the monomer droplets. On the other hand, Figure 2 represents the relationship between the monomer weight fraction in the polymer particles and that in the monomer droplets which are in equilibrium with the monomer-swollen particles. In this system, monomer droplets disappear from the water phase at a conversion between 32% and 43%, depending upon the weight fraction of MMA monomer in the monomer droplets which disappear due to absorption by the particles.

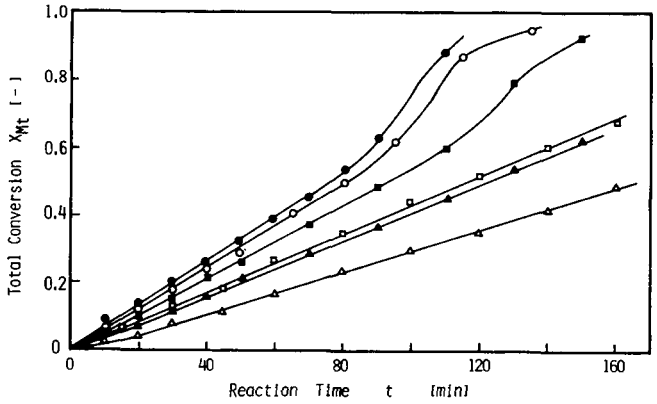

Fig. 3. Effect of initiator concentration on conversion vs. time history. Temp = 50°C; $N_T = 1.5 \times 10^{14}$ (particles/cm^3 water); $M_{m0} = 0.1$ (g/cm^3 water); $M_{s0} = 0.1$ (g/cm^3 water).

Key

	●	○	■	□	▲	△
$[I_0]$	6.25	2.50	1.25	0.50	0.313	0.125

Effect of Initiator Concentration on Copolymerization Rate

The average diameter and copolymer composition of the seed latex used in this series of copolymerization experiments were 55 nm and 0.5, respectively. Figure 3 exemplifies the total conversion of added monomer vs. reaction time observed when the number of polymer particles remained constant and the initial initiator concentration was varied. The conversion–time curves (Fig. 3) show almost straight lines at least from 10% to 50% conversions. From the slope of these straight lines, the copolymerization rate was calculated and plotted against initial initiator concentration (Fig. 4). The copolymerization rate increases with increasing initial initiator concentration. This emulsion copolymerization system does not obey the Smith–Ewart case II kinetic model, which predicts that the rate of emulsion polymerization does not increase with increasing initiator concentration if the number of polymer particles is constant. The dotted lines (Fig. 4) show the copolymerization rate calculated at the conversion where the seed particles have just absorbed all the monomer droplets present (about 36% conversion). In these calculations, eqs. (17), (18), (22), (23), and (11) were used, and the desorption of MMA-radicals from the particles was considered (k_{fm} = variable), but the desorption of ST-radicals was neglected (k_{fs} = 0) because, in styrene emulsion homopolymerization, radical desorption from the particles could be neglected under usual conditions. The values, k_{fm} = 0.5 and k_{fs} = 0 (Fig. 4), explain the observed copolymerization rate within experimental error. The solid line (Fig. 4) shows the rate of copolymerization calculated using eqs. (33) and (34) for estimating the values of k_{fm} and k_{fs}. On the other hand, the broken line (Fig. 4) represents those calculated using eq. (33) for k_{fm} and k_{fs} = 0. Both the solid and broken lines yield nearly identical values and agree well with the rate of copolymerization observed. This result also supports the validity of neglecting the desorption of ST-monomer radicals from the particles. Constants used in this calculation are listed in Table II. Most of them are literature values, but the values of δ_m and δ_s were estimated from those obtained by analyzing the emulsion homopolymerization of ST and MMA.[13] The values of C_{msm} and C_{mms} were determined so that the rates of copolymerization calculated can best explain those observed.

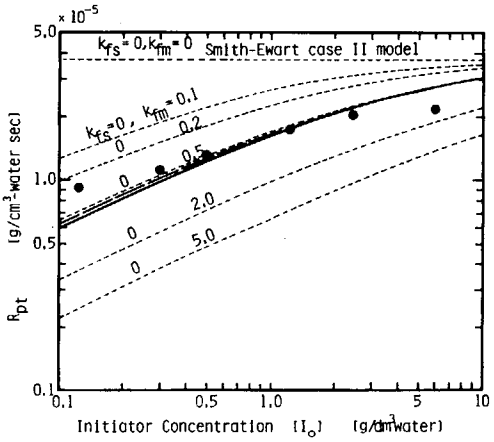

Fig. 4. Effect of initiator concentration on copolymerization rate observed and comparison with theory involving radical desorption from polymer particles. (---) k_{fw} = variable, k_{fs} = 0; (——) k_{fm} = eq. (33), k_{fs} = eq. (34); (– –) k_{fm} = eq. (33), k_{fs} = 0.

TABLE II
Numerical Values of Constants Used (50°C)

Const	Unit	Styrene (s)	Methyl methacrylate (m)
k_p	dm³/mol·s	210[a]	650[b]
γ	—	0.52[c]	0.46[c]
δ	—	0.2[d]	0.2[d]
C_m	—	$C_{mss} = 5 \times 10^{-5}$ [c]	$C_{mmm} = 2 \times 10^{-5}$ [c]
		$C_{msm} = 20 \times 10^{-5}$ [e]	$C_{mms} = 20 \times 10^{-5}$ [e]
m_d	—	1300[f]	50[f]
D_w	cm²/s	1.2×10^{-5} [g]	1.7×10^{-5} [g]
$k_d f$	1/s	$k_d f = 6.7 \times 10^{-7}$ [a] ($r_i = 2k_d f[I_0]_w$)	
$[M]_p$	mol/dm³-particles	Figures 1(a), 1(b) or eqs. (37) and (38)	

[a] From Harada et al.[14]
[b] From Mackay and Melville.[15]
[c] From *Polymer Handbook*.[16]
[d] From Nomura.[13]
[e] From this work.
[f] From Harada et al.[6]
[g] From Wilke and Chang.[17]

Effect of Particle Number on Copolymerization Rate

In Figure 5 are shown the conversion vs. time curves observed when the number of seed particles in the system was varied. In these runs, the total amount of monomer charged initially was increased in proportion to the number of seed particles in the system so that the variation of particle volume with conversion became the same in each run. The copolymerization rates was calculated from the slope of the conversion versus time curves (Fig. 5), and was plotted against the particle concentration (Fig. 6). The copolymerization rate observed is not proportional to the particle concentration. This emulsion copolymerization system does not follow the Smith–Ewart case II kinetic model. The dotted,

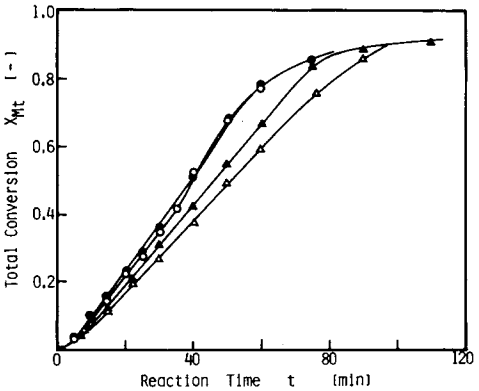

Fig. 5. Effect of particle number on conversion vs. time history. $[I_0] = 1.25$ (g/dm³ water); $M_{m0}/M_0 = 0.5$; temp = 50°C.

Key

	●	○	▲	△
N_T	0.5	1.0	2.0	4.0×10^{14}
M_0	0.025	0.05	0.10	0.20

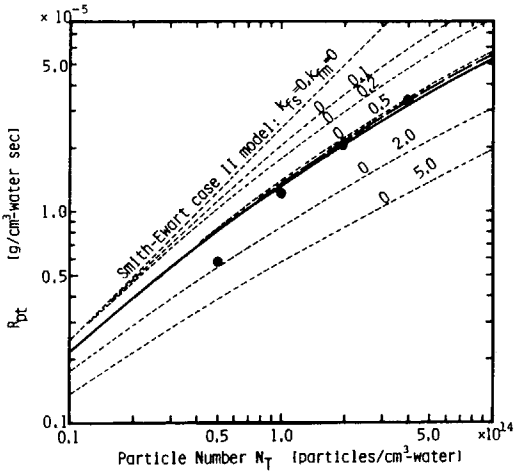

Fig. 6. Effect of particle number on copolymerization rate observed and comparison with theory involving radical desorption from polymer particles. (---) k_{fm} = variable, k_{fs} = 0; (——) k_{fm} = eq. (33), k_{fs} = eq. (34); (– –) k_{fm} = eq. (33), k_{fs} = 0.

broken, and solid lines (Fig. 6) are theoretical values calculated in the same manner as previously mentioned. The rate of copolymerization observed is in good agreement (Fig. 6) with that predicted theoretically except for the data at $N_T = 0.5 \times 10^{14}$ particles/cm^3 water. This data point deviates from the theoretical value as follows: The amount of MMA-monomer charged initially was 0.0125 g/cm^3 water, but this value is somewhat less than the solubility limit of MMA-monomer in water at 50°C (ca. 0.015 g/cm^3 water).[13] Thus, the concentration of MMA-monomer in the monomer-swollen particles was actually lower than the value which was estimated from Fig. 2 or eqs. (37) and (38), and was used for calculating the rate of copolymerization. Therefore, the rate of copolymerization observd in this condition becomes lower than that calculated.

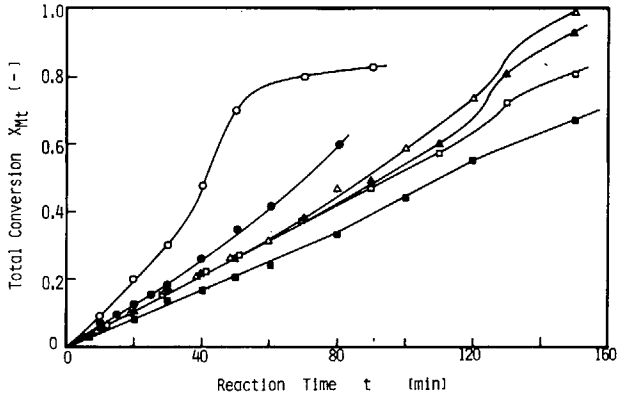

Fig. 7. Effect of initial monomer composition in monomer feed on conversion vs. time history. $N_T = 1.5 \times 10^{14}$ (particles/cm^3 water); $[I_0]$ = 1.25 (g/dm^3 water); temp = 50°C.

Key

	■	□	▲	△	●	○
M_{m0}/M_0	0.05	0.20	0.50	0.65	0.75	0.90

Effect of Comonomer Composition on Copolymerization Rate

Effect of comonomer composition on the copolymerization rate was examined by changing the comonomer composition in the monomer feed. Figure 7 shows the effect of monomer composition in the monomer feed on conversion versus time. When the weight fraction of MMA-monomer in the monomer feed is lower than about 0.7, the copolymerization rate becomes almost independent of the comonomer composition in the monomer feed, especially at lower conversion where monomer droplets exist in the water phase. The copolymerization rate increases sharply with increasing weight fraction of MMA-monomer in the monomer feed from about 0.7. The variation of the rate of copolymerization, which was calculated at about 35% conversion, with the weight fraction of MMA-monomer in the monomer feed, is presented (Fig. 8). Theoretical values are also plotted (Fig. 8) by the dotted, broken, and solid lines. The dotted line with the constant values $k_{fm} = 0.5$ and $k_{fs} = 0$ fits the observed value regardless of the change in the comonomer composition in the monomer feed. The solid line obtained by calculation using eqs. (33) and (34) for the prediction of the values of k_{fm} and k_{fs} explains the observed relationship between the copolymerization rate and the comonomer composition in the monomer feed. The broken line which shows the values calculated by neglecting only the desorption of ST-monomer radicals from the particles also explains the observed values accurately. Though experimental data are not shown here, during the interval where monomer droplets exist in the water phase, the comonomer composition in the monomer droplets was almost identical to that initially found in the monomer feed.

Effect of Particle Size on Copolymerization Rate

If radical desorption from the particles is important in this emulsion copolymerization system, it must be also demonstrated, as eqs. (27) and (33) predict, that, as the particle sizes becomes smaller, the copolymerization rate decreases due to an increase in the rate of radical desorption from the particles, even if the number of polymer particles present is constant. Seeded emulsion copoly-

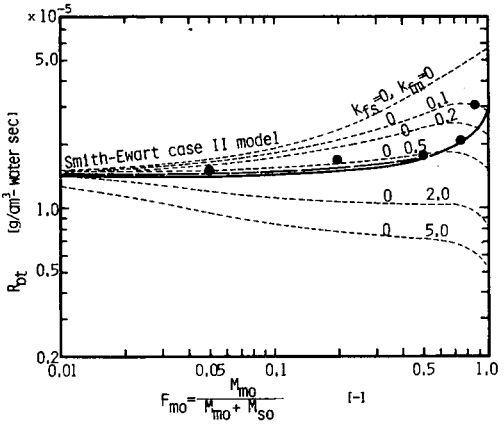

Fig. 8. Effect of initial monomer composition on copolymerization rate observed and comparison with theory involving radical desorption. (- - -) k_{fm} = variable, $k_{fs} = 0$; (——) k_{fm} = eq. (33), k_{fs} = eq. (34); (– –) k_{fm} = eq. (33), $k_{fs} = 0$.

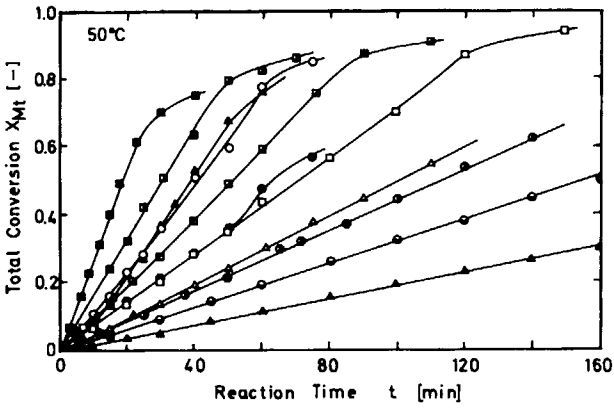

Fig. 9. Effect on conversion vs. time history of particle size changed by changing particle number and initial weight of total organic phase. $[I_0] = 1.25$ g/dm^3 water; $d_p = 40$ nm; $M_{m0}/M_0 = 0.5$.

Key

	■	◧	◪	□	○	●	◑	◒	▲	△	▲
W_0	0.063	0.113	0.213	0.313	0.053	0.103	0.203	0.303	0.027	0.102	0.301
$N_T \times 10^{-14}$	4.0	4.0	4.0	4.0	1.0	1.0	1.0	1.0	0.5	0.5	0.5

merization experiments were conducted to demonstrate this point. The particle size was changed by changing the number of seed particles in the system and the amount of monomer initially charged. The average particle volume ranged from 1.6×10^{-16} to 6.0×10^{-15} cm^3. The conversion vs. time curves observed in this series of experiments are shown in Figure 9, where W_0 is the initial weight of total organic phase consisting of polymer in the seed particles and monomer initially charged. The rate of copolymerization observed at about 35% conversion is shown in Figure 10. The values calculated with and without neglecting the desorption of ST-monomer radicals from the particles are also presented by the broken and solid lines (Fig. 10), corresponding to experimental conditions. The

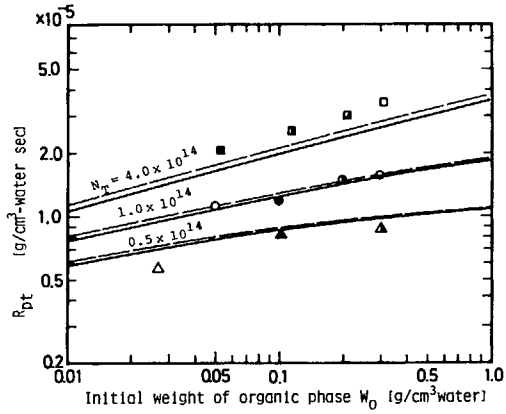

Fig. 10. Effect of particle size on copolymerization rate observed and comparison with theory involving radical desorption from polymer particles (corresponds to Fig. 9). $[I_0] = 1.25$ (g/dm^3 water); $M_{m0}/M_0 = 0.5$; (—) k_{fm} = eq. (33), k_{fs} = eq. (34); (– –) k_{fm} = eq. (33), $k_{fs} = 0$.

rate of copolymerization (Fig. 10) decreases with decreasing particle size due to an increase in the rate of radical desorption from the particles. The emulsion copolymerization model and the rate coefficient for radical desorption developed by the present authors explains the effect of particle size on the rate of emulsion copolymerization of ST and MMA.

CONCLUSION

It was clarified in this paper that: (1) The Smith–Ewart case II kinetic model does not explain the rate of emulsion copolymerization of ST and MMA, and this is due to radical desorption from the polymer particles; (2) the rate coefficient for radical desorption developed in this study and the emulsion copolymerization model proposed earlier by the present authors explain the rate of emulsion copolymerization of ST and MMA; (3) the desorption of MMA-monomer radicals (oligomer radicals) play an important role in determining the rate of emulsion copolymerization, while the desorption of ST-monomer radicals (oligomer radicals) can be neglected from a kinetic point of view; and (4) radical desorption from the particles does not affect the copolymer composition.

NOMENCLATURE

a_p	surface area of a particle (cm^2)
$C_{mab} = k_{mab}/k_{pab}$	chain transfer constant of A-radical to B-monomer
D_{wj} $(j = a, b)$	diffusion coefficient of j-monomer radicals in water (cm^2/s)
D_{pj} $(j = a, b)$	diffusion coefficient of j-monomer radicals in particles (cm^2/s)
d_p	diameter of a particle (cm)
F_{j0} $(j = a, b)$	initial weight fraction of j-monomer in the monomer feed
f	initiator efficiency
$[I]$	initiator concentration (g/dm^3 water or molecules/cm^3 water)
$[I_0]$	initial initiator concentration (g/dm^3 water or molecules/cm^3 water)
$[I^*]$	concentration of initiator radicals (mol/dm^3 water)
k_{fj} $(j = a, b, I)$	desorption rate coefficient for j-radicals (1/s)
k_d	rate constant for initiator decomposition (1/s)
k_{ij} $(j = a, b, I)$	initiation rate constant for j-radicals (dm^3/mol·s)
k_{ej} $(j = a, b, I)$	rate constant for radical entry into particles (dm^3 water/mol·(s)
K_{0j} $(j = a, b, I)$	desorption rate constant for j-monomer radicals (1/s)
k_{mab}	chain transfer rate constant of A-radical to B-monomer (dm^3/mol·s)
$\bar{k}_f$	average rate coefficient for radical desorption (1/s)
K_{sj} $(j = a, b, I)$	overall mass-transfer coefficient for j-monomer radical (cm/s)
k_{pab}	propagation rate constant of A-radical to B-monomer (dm^3/mol·s)
m_{dj} $(j = a, b, I)$	partition coefficient for j-radicals
M_j $(j = a, b)$	amount of j-monomer per unit water (molecules/cm^3 water or g/cm^3 water)
M_{jd} $(j = a, b)$	amount of j-monomer as monomer droplets (mol/cm^3 water or g/cm^3 water)
M_0	total amount of monomer charged initially (mol/cm^3 water or g/cm^3 water)
$[M_j]_k$ $(j = a, b,\ k = w, p)$	monomer concentration of j-monomer in the k phase (mol/dm^3 k phase)
$[M_j^*]_k$ $(j = a, b,\ k = w, p)$	concentration of j-monomer radicals in the k phase (mol/dm^3 k phase)
N_{jm}^* $(j = a, b, I)$	number of particles containing j-monomer (initiator) radical (particles/cm^3 water)
N_0	number of particles containing no radicals (particles/cm^3 water)

N_T	total number of particles (particles/cm^3 water)
$\bar{n}_j$ ($j = a, b, I$)	average number of j-radicals per particle (molecules/particle)
$\bar{n}_t$	average number of total radicals per particle (molecules/particle)
P_j ($j = a, b$)	amount of j-polymer in seed particles (g/cm^3 water)
r_i	rate of radical production (molecules/cm^3 water·s)
R_{pj} ($j = a, b$)	polymerization rate for j-monomer (mol/cm^3 water·s or g/cm^3 water·s)
R_{pt}	total polymerization rate (mol/cm^3 water·s or g/cm^3 water·s)
v_p	volume of a particle (cm^3)
X_{Mj} ($j = a, b$)	conversion of j-monomer to polymer
X_{Mt}	total conversion of monomer to polymer
w_{fj} ($j = a, b$)	weight fraction of j-monomer in monomer droplets
W_0	initial weight of total organic phase (g/cm^3 water)

Greek Letters

Φ_{Mj} ($j = a, b$)	probability of j-monomer radicals escaping from particles before adding one monomer unit
ρ_p	density of polymer particles (g/cm^3)
γ_j ($j = a, b$)	reactivity ratio of j-monomer
μ	ionic strength in the water phase
σ	surface tension of seed latex (dyn/cm)
δ_j ($j = a, b$)	ratio of water-side mass-transfer resistance to overall mass-transfer resistance for j-monomer radicals

Subscripts

a	A-monomer
b	B-monomer
p	particle phase
w	water phase
I	initiator
m	MMA-monomer
s	ST-monomer
0	initial value

References

1. C. C. Lin, H. C. Ku, and W. Y. Chiu, *J. Appl. Polym. Sci.*, **26**, 1327 (1981).
2. (a) M. Nomura, K. Yamamoto, K. Fujita, M. Harada, and W. Eguchi, preprints of the 12th Fall Meeting of the Society of Chemical Engineers of Japan, Okayama, Japan. G8-207, 1978, p. 439; (b) M. Nomura, *Int. Polym. Colloid Group Newsletter*, 8(2), (1978); (c) M. Nomura, K. Yamamoto, K. Fujita, M. Harada, and W. Eguchi, preprints of the 3rd International Conference on Surface and Colloid Sciences, August 20–25, 1979, Stockholm, Sweden, p. 148.
3. M. J. Ballard, D. H. Napper, and R. G. Gilbert, *J. Polym. Sci., Polym. Chem. Ed.*, **19**, 939 (1981).
4. M. Litt, R. Patsiga, and V. Stannett, *J. Polym. Sci., Part A-1*, **8**, 3607 (1970).
5. (a) J. Ugelstad, P. C. Mørk, P. Dahl, and P. Rangnes, *J. Polym. Sci., Part C*, **27**, 49 (1969); (b) J. Ugelstad and P. C. Mørk, *Br. Polym. J.* **2**, 31 (1970).
6. M. Harada, M. Nomura, W. Eguchi, and S. Nagata, *J. Chem. Eng. Jpn.*, **4**, 54 (1971).
7. N. Friis, and M. Nyhagen, *J. Appl. Polym. Sci.*, **17**, 1973).
8. M. Nomura, and M. Harada, *J. Appl. Polym. Sci.*, **26**, 17 (1981).
9. M. Nomura, in *Emulsion Polymerization*, I. Piirma, Ed., Academic, New York, 1982, Chap. 5, pp. 191–219.
10. M. Nomura, M. Kubo, and K. Fujita, *Mem. Fac. Eng. Fukui Univ.*, **29**(2), 167 (1981).
11. M. Nomura, M. Harada, W. Eguchi, and S. Nagata, in *Emulsion Polymerization*, I. Piirma and J. L. Gardon, Eds., ACS Symposium Series No. 24, American Chemical Society, Washington, D.C., 1976, pp. 102–122.

12. K. Chang, M. Litt, and M. Nomura, in *Emulsion Polymerization of Vinyl Acetate*, M. S. El-Aasser & J. W. Vanderhoff, Eds., Applied Science Publishers, London and New Jersey, 1981, Chap. 6, pp. 89–136.

13. M. Nomura, unpublished results.

14. M. Harada, M. Nomura, H. Kojima, W. Eguchi, and S. Nagata, *J. Appl. Polym. Sci.*, **16**, 811 (1972).

15. M. H. Mackay and H. W. Melville, *Trans. Faraday Soc.*, **45**, 323 (1949).

16. J. Brandrup and E. H. Immergut, Eds., *Polymer Handbook*, 2nd ed., II-59, Wiley, New York, 1975.

17. C. R. Wilke and P. C. Chang, *AIChE J.*, **1**, 264 (1955).

Received October 10, 1981
Accepted January 4, 1982